Parametric scattering of microcavity polaritons into ghost branches

Joanna M Zajac* and Wolfgang Langbein
School of Physics and Astronomy, Cardiff University,
The Parade, Cardiff CF24 3AA, United Kingdom
(Dated: April 20, 2013)

Polaritons of defined momentum and energy are excited resonantly on the lower polariton branch of a planar semiconductor microcavity in the strong coupling regime, and the spectrally and momentum resolved emission is analyzed. We observe ghost branches from scattering within the lower polariton branch, as well as from scattering to the middle polariton branch, showing the non-linear mixing between different branches. Extending the theoretical treatment of spontaneous parametric luminescence developed in Ciuti *et al.*, Phys. Rev. B **63**, 041303 (2001), the eigenmodes of the driven polariton system and its photoluminescence are modeled. A quantitative agreement with the measured branch positions and a qualitative agreement with the branch intensities is found.

Cavity excitons-polaritons in planar semiconductor microcavities are quasi-particles resulting from strong coupling between the Fabry-Pérot cavity mode and excitonic resonance of the semiconductor inside the cavity. Below the exciton saturation density, polaritons can be treated as composite bosons[1]. They inherit features of exciton and photon constituents resulting in strong interactions from the exciton and steep in-plane dispersion and propagation from the cavity mode. The parametric scattering of microcavity polaritons is described in lowest order by the third-order susceptibility[2]. Given a coherent population of 'pump' (P) polaritons, which are scattered into 'signal' (S) and 'idler' (I) polaritons, the phase matching in time and space results in the conservation of energy $2E_{\mathrm{P}} = E_{\mathrm{S}}+E_{\mathrm{I}}$, and momentum $2\mathbf{k}_{\mathrm{P}} = \mathbf{k}_{\mathrm{S}}+\mathbf{k}_{\mathrm{I}}$, where $\mathbf{k}$ is the wavevector. The scattering is resonant to the eigenstates of the system, which in the investigated sample are the polaritons of the lower, middle and upper branches with the energies $E_{\mathrm{LP}}(\mathbf{k}), E_{\mathrm{MP}}(\mathbf{k}), E_{\mathrm{UP}}(\mathbf{k})$. This scattering enables optical parametric amplification[3]. Self-seeded multiple parametric scattering into real and ghost branches of the lower polariton branch under pulsed and steady state pumping was reported in Ref. 4,5, respectively. Transient seeded scattering into real and ghost branches of the lower polariton was reported in Ref. 6. A theoretical model of the spontaneous parametric fluorescence was developed in Ref. 7, and extended to stimulated emission in Ref. 8. This model uses a Bogoliubov formalism to describe scattering from a macroscopically occupied pump state and neglects quantum fluctuations of the pump state. Spontaneous parametric emission was experimentally investigated in Ref. 9,10 showing scattering into the phase-matched 8-shapes in momentum space, which was then demonstrated to provide entangled photon sources[10,11], which was recently realized also in one-dimensional cavity structures[12,13]. We believe that in order to qualitatively analyze dynamics of quantum fluids[14] or multiple-quantum fluids[15,16] of cavity polaritons, real-space measurements should be accompanied by k-resolved measurement, as discussed here, what would undoubtedly indicate the quantum state of polariton fluids.

In this letter, we report on spontaneous parametric scattering of resonantly injected polaritons under steady state pumping. We observe scattering from the macroscopically populated pump state into real and ghost branches of the lower and middle polariton in two-dimensional momentum space. Theoretical predictions of the scattering using an extension of Ref. 7 show a good agreement with the measurements.

The microcavity sample[17] investigated here is a 1λ $\mathrm{Al_{0.05}Ga_{0.95}As}$ cavity with a single 15 nm GaAs quantum well with 5 nm $\mathrm{Al_{0.3}Ga_{0.7}As}$ barriers in its center, providing two excitonic resonances, the heavy hole and the light hole exciton. The cavity is surrounded by $\mathrm{AlAs/Al_{0.15}Ga_{0.85}As}$ distributed Bragg reflectors with 25(16) periods on the bottom(top) of the epilayer. The cavity mode energy gradient was about 1.5 meV/mm, which allowed to adjust the detuning between cavity and heavy-hole exciton $\Delta_{\mathrm{c}} = E_{\mathrm{c}} - E_{\mathrm{hh}}$. The use of a wide binary GaAs well eliminates the alloy disorder found in InGaAs/GaAs quantum wells[18], resulting in an inhomogeneous exciton linewidth of[17] 170 μeV. The $\mathrm{Al_{0.05}Ga_{0.95}As}$ cavity reduces the carrier confinement and thus the carrier trapping and the related homogenous broadening[19]. The resulting exciton linewidth was measured here at full-width half maximum as $\gamma_{\mathrm{hh}} = 150\,\mu$eV using reflection spectroscopy. The cavity linewidth γ_{c} of about $300\,\mu$eV is limited by the reflectivity of the top Bragg mirror.

The sample was mounted in a helium bath cryostat at a temperature of 5 K and a vapor pressure of 200 mbar. To measure the polariton dispersion, we used a weak pulsed excitation with a mode-locked Ti:Sapphire laser (Coherent Mira) delivering 100 fs pulses at 76 MHz repetition rate and a spectral width of approximately 20 meV. The excitation was focused to a diffraction limited spot of $1.5\,\mu$m with a 0.5NA lens having a wavevector range of $|k| \leq 4/\mu$m. To excite pump polaritons for parametric scattering, we used a linearly polarized single-mode CW external cavity diode laser with a spectral width of 20 neV. Two-dimensional excitation wavevector control was achieved by imaging collimated laser beam ($\simeq$2 mm diameter) onto the gimbal mirror[9], from there laser spot was demagnified by a factor of 38 and imaged onto the sample. The beam divergence at the mirror was adjusted to create a gaussian tail at the sample, providing the minimum wavevector spread for a given excitation size. The beam diameter at $1/e$ intensity on the sample was $70\,\mu$m, corresponding to a wavevector spread of $|\mathbf{k}| \leq 0.09/\mu$m. In order to avoid sample heating, the excitation was chopped by an acousto-optic modulator producing pulses

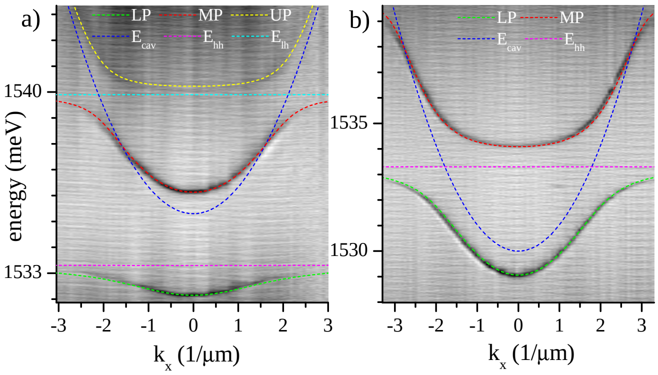

FIG. 1: Reflection of the microcavity as function of photon energy and wavevector $\mathbf{k} = (k_x, 0)$. a) positive detuning $\Delta_c = 5\,\mathrm{meV}$. b) negative detuning $\Delta_c = -4\,\mathrm{meV}$. The calculated polariton dispersions $\tilde{E}_B(\mathbf{k})$ are given by lines as labeled.

of $1\,\mu$s pulse duration at 1% duty cycle. The peak intensity on the sample I was about $10^3\,\mathrm{W/cm^2}$. The resonantly created polariton density $N_{\mathrm{LP}}(\mathbf{k}_\mathrm{P}) \simeq I\tau T/E_\mathrm{P} \simeq 10^7/\mathrm{cm}^2$ [26], the The reciprocal space ($\mathbf{k}$) of the cross-linearly polarized emission was imaged onto the input slit of a high resolution ($20\,\mu$eV) imaging spectrometer and detected using a CCD-Camera[20,21]. The polariton dispersion in the low-intensity regime was measured using $\mathbf{k}$ resolved reflection spectroscopy as shown in Fig. 1, and modeled with the coupled three oscillator model for the cavity mode, heavy- and light-hole exciton[19,22]. From these fits of $E_\mathrm{B}(\mathbf{k})$ to the set of polariton branches B={LP,MP,UP}, we deduced the exciton energies $E_{\mathrm{hh}} = 1.5333\,\mathrm{eV}$, $E_{\mathrm{lh}} = 1.5399\,\mathrm{eV}$, and the Rabi splittings $2\,\Omega_{\mathrm{hh}} = 3.7\,\mathrm{meV}$, $2\,\Omega_{\mathrm{lh}} = 2.4\,\mathrm{meV}$, for heavy- and light-hole excitons, respectively. The exciton and polariton linewidths of this sample were previously compared[17] with the linewidth averaging model, in which the polariton linewidth γ_B is a weighted average of γ_c and the exciton linewidths $\gamma_{\mathrm{hh}}, \gamma_{\mathrm{lh}}$,

$$\gamma_\mathrm{B} = x_{\mathrm{lh,B}}\gamma_{\mathrm{hh}} + x_{\mathrm{lh,B}}\gamma_{\mathrm{lh}} + c_\mathrm{B}\gamma_\mathrm{c} \tag{1}$$

with the contents of cavity c_B, heavy hole exciton $x_{\mathrm{hh,B}}$, and light hole exciton $x_{\mathrm{lh,B}}$ in the polariton[23]. The model is assuming Lorenzian lineshapes, and shows sufficient agreement[17] with the experiment for the LP at zero and negative detuning. Increasing the exciton density as relevant in our experiments, the exciton linewidth is dominated by exciton-exciton scattering, which has a different non-Lorentzian shape compared to inhomogeneous broadening.

The parametric emission was modeled following Ref. 7, where the polaritons are excited resonantly with a pump field $P_\mathrm{P}(t) = \langle p^\dagger_{\mathrm{LP}}(\mathbf{k}_\mathrm{P}, t)\rangle$ of defined wavevector $\mathbf{k}_\mathrm{P}$ and photon energy E_P within the LP branch. The polaritons of signal and idler are coupled by a momentum conserving exciton-exciton scattering proportional to the pump intensity, described by off-diagonal terms in an anti-hermitian coupling matrix. In the following we use the renormalised complex polariton energies $\widehat{E}_\mathrm{B} = E_\mathrm{B} - i\gamma_\mathrm{B} + E^{\mathrm{ren}}_\mathrm{B}|P_\mathrm{P}|^2$. The polariton-polariton interaction term $E^{\mathrm{ren}}_\mathrm{B}$ was determined using Eq. 9 in Ref. 9

$$E^{\mathrm{ren}}_\mathrm{B}(\mathbf{k}) = 2x_{\mathrm{LP}}(\mathbf{k}_\mathrm{P})x_\mathrm{B}(\mathbf{k})\,\{12E_\mathrm{X} + \frac{16\pi}{7}\Omega_{\mathrm{hh}}\left[\sqrt{x^{-1}_{\mathrm{LP}}(\mathbf{k}_\mathrm{P}) - 1} + \sqrt{x^{-1}_\mathrm{B}(\mathbf{k}) - 1}\right]\Bigg\}, \tag{2}$$

with an exciton binding energy of $E_\mathrm{X} = 8\,\mathrm{meV}$. The excitonic content x_B was taken as the sum $x_\mathrm{B} = x_{\mathrm{hh,B}} + x_{\mathrm{lh,B}}$ of heavy and light hole content. The expression holds for circular polarization, so that for the cross-linear polarization configuration used here in the regime where the renormalisation is smaller than the linewidth we expect some deviations in the overall scattering strength. For higher polariton densities the spin-dependent interaction is influencing the dynamics significantly[24].

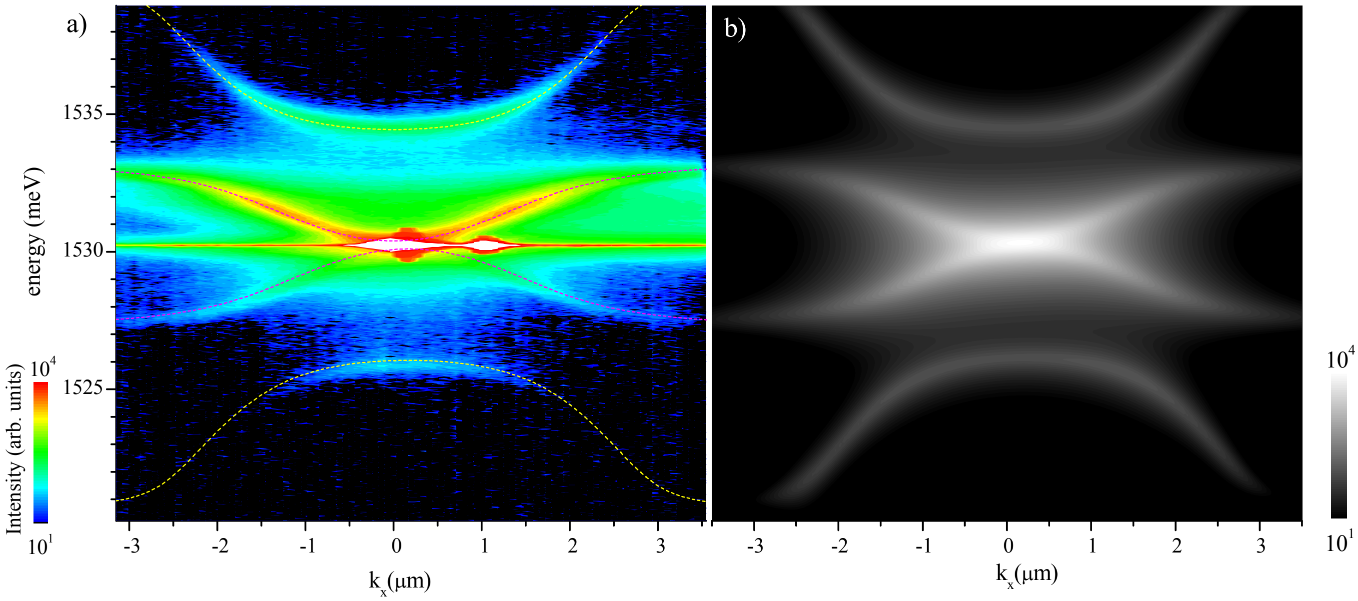

FIG. 2: Energy and wavevector resolved emission intensity $I(\mathbf{k},\omega)$ on a logarithmic scale as indicated, for a pump energy $E_{\mathrm{P}} = 1530.25\,\mathrm{meV}$ and wavevector $\mathbf{k}_{\mathrm{P}} = (0.1, 0)/\mu\mathrm{m}$ at a cavity detuning of $\Delta_{\mathrm{c}} = -1.7\,\mathrm{meV}$, injected polariton density $N_{\mathrm{LP}}(\mathbf{k}_{\mathrm{P}}) = 2.23 \cdot 10^7$. a) Measured $I(\mathbf{k},\omega)$ for $\mathbf{k} = (k_x, 0.4/\mu\mathrm{m})$. Lines: Eigenmodes $\widehat{E}^{\pm}_{\mathrm{B}}(\mathbf{k})$ of Eq.(3), for B=LP in magenta, and for B=MP in yellow. b) Parametric emission $I^{\mathrm{par}}(\mathbf{k},\omega)$ calculated using Eq.(5). The same dynamic ranges of the data were plotted for all figures shown hereafter. Horizontal line at E_{P} is due to the saturation of CCD-camera pixels at the laser energy.

Neglecting higher-order scattering processes and Langevin terms of the external light field, the steady-state emission from these branches was derived in an analytical form (Eq. 9 of Ref. 7) as a function of the steady state population of the signal $N_{\rm B}(\mathbf{k}_{\rm S}) = \langle p^\dagger_{\rm B}(\mathbf{k}_{\rm S},0)p_{\rm B}(\mathbf{k}_{\rm S},0)\rangle$ and an anomalous parametric correlation amplitude between signal and idler polaritons $A^*_{\rm B}(\mathbf{k}_{\rm S}) = \langle p^\dagger_{\rm B}(\mathbf{k}_{\rm S},0)p^\dagger_{\rm B}(\mathbf{k}_{\rm I},0)\rangle$ where $p_{\rm B}(\mathbf{k},t)$ is the time-dependent polariton operator of branch B and wavevector $\mathbf{k}$. We extended the model to include the middle polariton branch (MP) resulting in a corresponding ghost branch (MP*). The coupling matrix for the different branches is given by

$$M^{\rm par}_{\rm B} = \begin{pmatrix} \widehat{E}_{\rm B}(\mathbf{k}_{\rm S}) & E^{\rm int}_{\rm B}P^2_{\rm P} \\ -(E^{\rm int}_{\rm B}P^2_{\rm P})^* & 2E_{\rm P}-\widehat{E}^*_{\rm B}(\mathbf{k}_{\rm I}) \end{pmatrix} \qquad (3)$$

having the eigenvalues $\widehat{E}^{\pm}_{\rm B}(\mathbf{k}_{\rm S})$. The interaction energy $E^{\rm int}_{\rm B}$ is given by Eq. 8 in Ref. 9,

$$\begin{aligned} E^{\rm int}_{\rm B}(\mathbf{k}_{\rm S}) \;=\; & x_{\rm LP}(\mathbf{k}_{\rm P})\sqrt{x_{\rm B}(\mathbf{k}_{\rm S})x_{\rm B}(\mathbf{k}_{\rm I})} \times \qquad (4)\\ & \left\{12E_{\rm X} + \frac{16\pi}{7}\Omega_{\rm hh}\left[2\sqrt{x^{-1}_{\rm LP}(\mathbf{k}_{\rm P})-1}+\right.\right.\\ & \left.\left.\sqrt{x^{-1}_{\rm B}(\mathbf{k}_{\rm S})-1}+\sqrt{x^{-1}_{\rm B}(\mathbf{k}_{\rm I})-1}\right]\right\}, \end{aligned}$$

The parametric emission intensity of each polariton branch $I^{\rm par}_{\rm B}$ is then given by

$$\begin{aligned} & I^{\rm par}_{\rm B}(\mathbf{k}_{\rm S},\omega) \propto c_{\rm B}(\mathbf{k}_{\rm S}) \times \qquad (5)\\ & \Im\left\{\frac{\Delta_{\rm B}(\mathbf{k}_{\rm S},\omega)N_{\rm B}(\mathbf{k}_{\rm S}) + E^{\rm int}_{\rm B}(\mathbf{k}_{\rm S})P^2_{\rm P}A^*_{\rm B}(\mathbf{k}_{\rm S})}{\left(\widehat{E}^{+}_{\rm B}(\mathbf{k}_{\rm S})-\hbar\omega\right)\left(\hbar\omega-\widehat{E}^{-}_{\rm B}(\mathbf{k}_{\rm S})\right)}\right\} \end{aligned}$$

with

$$A_{\rm B}(\mathbf{k}_{\rm S}) = \frac{E^{\rm int}_{\rm B}(\mathbf{k}_{\rm S})P^2_{\rm P}\delta_{\rm B}(\mathbf{k}_{\rm S})}{|\delta_{\rm B}(\mathbf{k}_{\rm S})|^2 - \frac{(\gamma_{\rm B}(\mathbf{k}_{\rm S})+\gamma_{\rm B}(\mathbf{k}_{\rm I}))^2}{\gamma_{\rm B}(\mathbf{k}_{\rm S})\gamma_{\rm B}(\mathbf{k}_{\rm I})}\left|E^{\rm int}_{\rm B}(\mathbf{k}_{\rm S})P^2_{\rm P}\right|^2},$$

$N_{\rm B}(\mathbf{k}_{\rm S}) = \Im\left\{E^{\rm int}_{\rm B}(\mathbf{k}_{\rm S})P^2_{\rm P}A^*_{\rm B}(\mathbf{k}_{\rm S})\right\}/\gamma_{\rm B}(\mathbf{k}_{\rm S})$, the emission detuning $\Delta_{\rm B}(\mathbf{k}_{\rm S},\omega) = \hbar\omega + \widehat{E}^*_{\rm B}(\mathbf{k}_{\rm I}) - 2E_{\rm P}$ and the signal-idler detuning $\delta_{\rm B}(\mathbf{k}_{\rm S}) = 2E_{\rm P} - \widehat{E}^*_{\rm B}(\mathbf{k}_{\rm S}) - \widehat{E}^*_{\rm B}(\mathbf{k}_{\rm I})$. The total emission $I^{\rm par}$ is the sum of $I^{\rm par}_{\rm B}$ over all branches B. This theoretical treatment is valid below the threshold for parametric oscillation given by the condition $\Im(\widehat{E}^{-}_{B}(\mathbf{k}_{\rm S})) < 0$. We used the complex polariton energies $\widehat{E}_{\rm B}$ calculated in the three coupled oscillator model with a k-dependent broadening from Eq.(1) with $\gamma_{\rm c} = 300\mu$eV and $\gamma_{\rm lh} = \gamma_{\rm hh} = 400\mu$eV. The exciton linewidths are higher than measured in the low intensity regime, which we attribute to exciton-exciton scattering by the higher exciton density in the parametric scattering experiments[25]. The pump is assumed to be resonant to the LP branch. The simulations shown are well below the threshold, for which the renormalisation is small $E^{\rm ren}_{\rm B} \sim 10\,\mu$eV and the polariton density is $N_{\rm LP}(\mathbf{k}_{\rm P}) \sim 10^7/{\rm cm}^2$. In this regime, $I^{\rm par}$ is independent of the pump intensity up to a scaling factor. The simulations were made with a step size of $20\,\mu$eV in $\hbar\omega$ and $0.06/\mu$m in $\mathbf{k}_{\rm S}$.

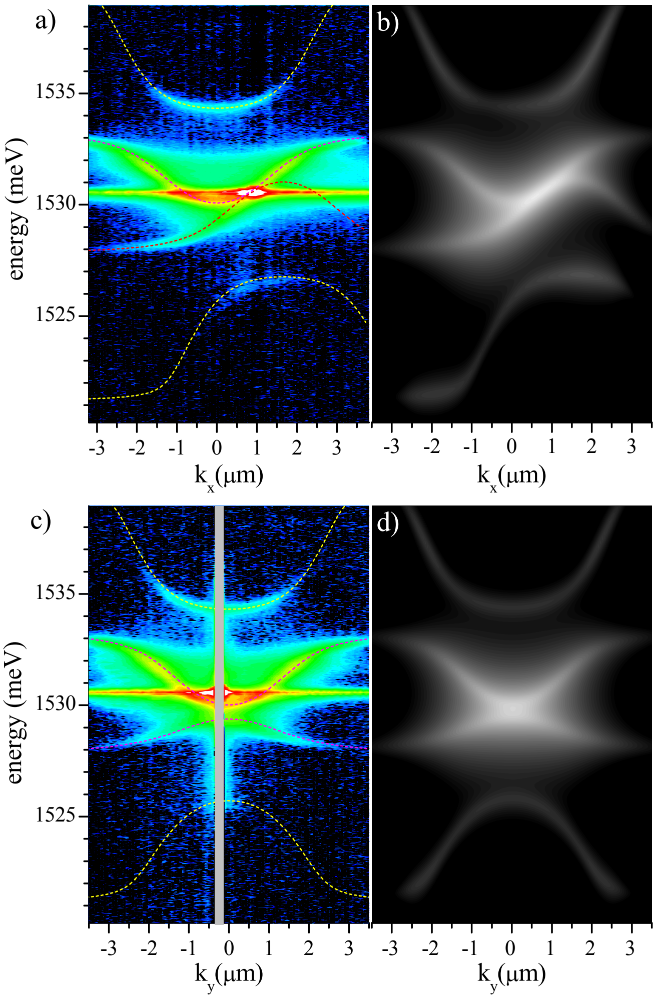

FIG. 3: As Fig. 2, but for $E_{\rm P} = 1530.55$ meV, $\mathbf{k}_{\rm P} = (0.85,0)/\mu$m, $\Delta_{\rm c} = -2.1$ meV, injected polariton density $N_{\rm LP}(\mathbf{k}_{\rm P}) = 2.18\cdot 10^7$. a,b) $\mathbf{k} = (k_x, 0.3/\mu{\rm m})$. c,d) $\mathbf{k} = (0/\mu{\rm m}, k_y)$.

We now discuss the measured microcavity emission for different pump energies and wavevectors together with corresponding results of simulations. We commence with a pump close to the dispersion minimum at $E_{\rm P} = 1530.15$ meV and $\mathbf{k}_{\rm P} = (0.1,0)/\mu$m for a cavity detuning $\Delta_{\rm c} = -1.7$ meV, shown in Fig. 2. The measured emission $I((k_x, 0.4/\mu{\rm m}),\omega)$ shown in Fig. 2a shows the dominant emission from the LP and from the pump which is scattered elastically by disorder towards the detection wavevector range. The emission from the MP is about 2 orders of magnitude weaker, and the ghost branches LP* and MP* are 2-4 orders of magnitude weaker and show a reversed dispersion. The corresponding predicted eigenvalues $\widehat{E}^{\pm}_{\rm B}(\mathbf{k})$ of Eq.(3) are following the observed emission peaks. For a more detailed comparison with theory, we give in Fig. 2b the calculated parametric emission intensity $I^{\rm par}$, which shows a semi-quantitative agreement with the experimental result. The main deviation is the observed intensity of the ghost branches, which in the experiment is much weaker than in the simulation. This is actually expected as the model accounts for radiative broadening only, such that all parametrically scattered

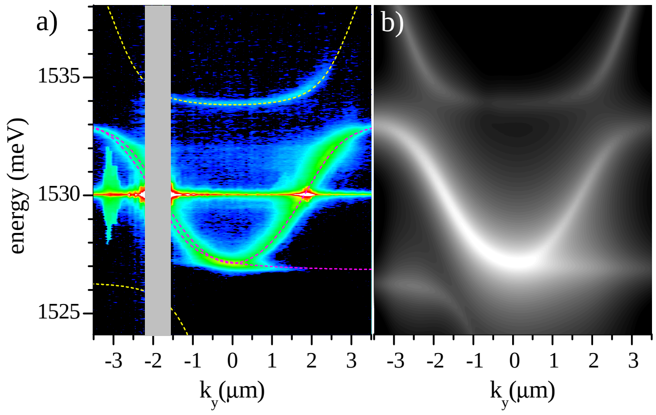

FIG. 4: As Fig. 2, but for $E_\mathrm{P} = 1530.1\,\mathrm{meV}$, $\mathbf{k}_\mathrm{P} = (0, -1.9)/\mu\mathrm{m}$, $\Delta_\mathrm{c} = -5.5\,\mathrm{meV}$, injected polariton density $N_\mathrm{LP}(\mathbf{k}_\mathrm{P}) = 2.05 \cdot 10^7$ and cross-section $\mathbf{k} = (0, k_y)$.

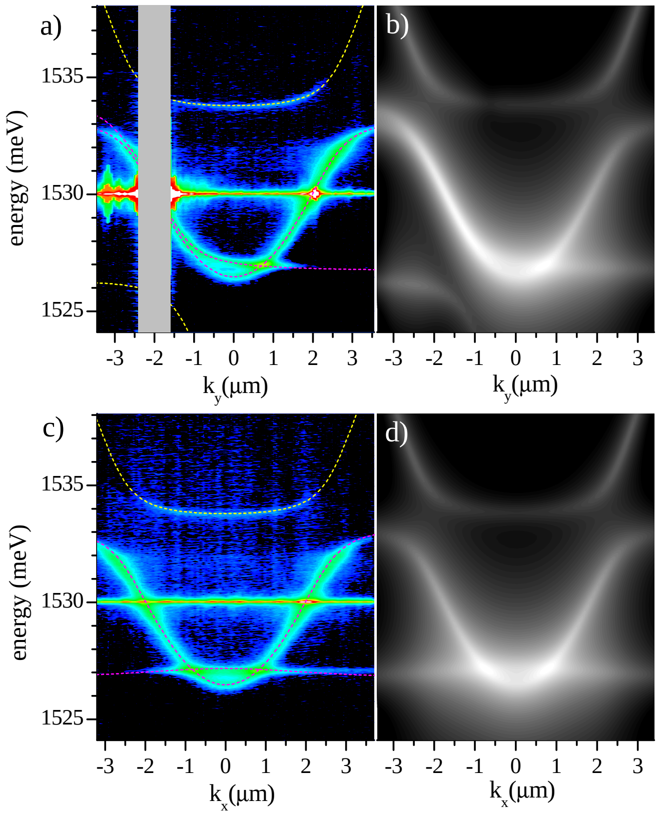

FIG. 5: As Fig. 2 but for $E_\mathrm{P} = 1530.0\,\mathrm{meV}$, $\mathbf{k}_\mathrm{P} = (0, -1.95)/\mu\mathrm{m}$, $\Delta_\mathrm{c} = -6\,\mathrm{meV}$, injected polariton density $N_\mathrm{LP}(\mathbf{k}_\mathrm{P}) = 2.05 \cdot 10^7$ and $\mathbf{k} = (-0.25/\mu\mathrm{m}, k_y)$ for a,b and $\mathbf{k} = (k_x, 0)$ in (c,d).

polaritons are emitted, resulting in equal intensities of signal and idler. In the experiment, a significant part of the broadening at higher $\mathbf{k}$ is due to the exciton linewidth (see Eq.(1)), which represents a scattering of polaritons into excitonic states. This scattering results in a thermalized population of excitons at high $\mathbf{k}$, emitting dominantly from the LP and the bottleneck region, which is the reason for the observed strong LP emission. Ghost branches are best visible for small $\mathbf{k}_\mathrm{P}$ due to the smaller contribution of the exciton broadening[25].

Moving the pump away from the dispersion minimum to $\mathbf{k}_\mathrm{P} = (0.85, 0)/\mu\mathrm{m}$, the emission reveals the expected asymmetry as shown in Fig. 3. Two different cross-sections $\mathbf{k} = (k_x, 0.3/\mu\mathrm{m})$ in (a,b) and $\mathbf{k} = (0/\mu\mathrm{m}, k_y)$ in (c,d) of the full three-dimensional data set are given.

Moving further along the dispersion to $\mathbf{k}_\mathrm{P} = (0, -1.9)/\mu\mathrm{m}$ close to the inflexion point, as shown in Fig. 4, LP and LP* intersect close to the dispersion minimum at $\mathbf{k}_\mathrm{P} = (0, -0.5)/\mu\mathrm{m}$ and $\mathbf{k}_\mathrm{P} = (0, 0.2)/\mu\mathrm{m}$, at which energy and momentum conserving scattering is resonant for signal and idler. This pump wavevector is close to the so-called magic angle[3] for which LP and LP* intersect at $\mathbf{k} = 0$ resulting in a small threshold for parametric oscillation. For this excitation the ghost branches are visible mainly at the intersection points. This could partly be due to the onset of stimulated scattering[23]. The corresponding simulations shown in Fig. 4b give good agreement with measurement for the LP branch. However, the calculated MP branch has a weaker emission for small $\mathbf{k}$, and a higher emission for large $\mathbf{k}$. This is again related to the exciton scattering into the exciton reservoir and subsequent emission of thermalized excitons, as the middle polariton the highest exciton content at small $\mathbf{k}$.

In Fig. 5, we show measured polariton luminescence for $\mathbf{k}_\mathrm{P} = (0, -1.95)/\mu\mathrm{m}$ well above the inflexion point, resulting in an 8-shaped resonant region[9] in $\mathbf{k}$ space. In the cross-section $\mathbf{k} = (-0.25/\mu\mathrm{m}, k_y)$, the LP real and ghost branches intersect at $E = 1526.95\,\mathrm{meV}, \mathbf{k} = (-0.25, 0.7)/\mu\mathrm{m}$. In the cross-section $\mathbf{k} = (k_x, 0)$ shown in Fig. 5c, the LP real and ghost branches intersect at $E = 1527.1\mathrm{meV}$, $\mathbf{k} = (\pm 0.82, 0)/\mu\mathrm{m}$. Again a good agreement with the simulations is found.

In summary we have shown polariton parametric pair scattering from a resonantly excited pump state into real and ghost branches of signal and idler polaritons for different excitation angles and wavevectors. The measurements are in agreement with simulations, apart from the additional emission due to thermalized excitons related to the missing treatment of non-radiative scattering processes. These results can be further explored towards entangled photon source by measurements of their time-correlation, measurements for higher pump powers which will give rise to stronger renormalisation and deviation of polariton dispersion from quadratic can be also studied.

Acknowledgments

This work was supported by the EPSRC under grant n. EP/F027958/1.

---

* Electronic address: `joanna.m.zajac@gmail.com`

[1] A. Kavokin, J. Baumberg, G. Malpuech, and F. Laussy,

Microcavities, Series on Semiconductor Science and Technology (OUP Oxford, 2007), ISBN 9780191620737.

[2] R. W. Boyd, *Nonlinear Optics* (Academic Press, 2008).

[3] P. G. Savvidis, J. J. Baumberg, R. M. Stevenson, M. S. Skolnick, D. M. Whittaker, and J. S. Roberts, Phys. Rev. Lett. **84**, 1547 (2000).

[4] P. G. Savvidis, C. Ciuti, J. J. Baumberg, D. M. Whittaker, M. S. Skolnick, and J. S. Roberts, Phys. Rev. B **64**, 075311 (2001).

[5] A. I. Tartakovskii, D. N. Krizhanovskii, D. A. Kurysh, V. D. Kulakovskii, M. S. Skolnick, and J. S. Roberts, Phys. Rev. B **65**, 081308 (2002).

[6] V. Kohnle, Y. Léger, M. Wouters, M. Richard, M. T. Portella-Oberli, and B. Deveaud-Plédran, Phys. Rev. Lett. **106**, 255302 (2011).

[7] C. Ciuti, P. Schwendimann, and A. Quattropani, Phys. Rev. B **63, 4**, 5 (2001), parametric.

[8] C. Ciuti, P. Schwendimann, and A. Quattropani, Semicond. Sci. Technol. **18**, S279 (2003).

[9] W. Langbein, Phys. Rev. B **70**, 205301 (2004).

[10] W. Langbein, Phys. Status Solidi B **242**, 2260 (2005).

[11] S. Savasta, O. D. Stefano, V. Savona, and W. Langbein, Phys. Rev. Lett. **94**, 246401 (2005).

[12] M. Abbarchi, V. Ardizzone, T. Lecomte, A. Lemaitre, I. Sagnes, P. Senellart, J. Bloch, P. Roussignol, and J. Tignon, Phys. Rev. B **83**, 201310 (2011).

[13] V. Ardizzone, M. Abbarchi, T. Lecomte, A. Lemaitre, I. Sagnes, P. Senellart, J. Bloch, P. Roussignol, and J. Tignon, Phys. Status Solidi B **249**, 896 (2012).

[14] A. Amo, J. Lefrere, S. Pigeon, C. Adrados, C. Ciuti, I. Carusotto, R. Houdré, E. Giacobino, and A. Bramati, Nature Physics **5**, 805 (2009).

[15] E. Cancellieri, F. M. Marchetti, M. H. Szymańska, D. Sanvitto, and C. Tejedor, Phys. Rev. Lett. **108**, 065301 (2012).

[16] D. Ballarini, M. D. Giorgi, E. Cancellieri, R. Houdré, E. Giacobino, R. Cingolani, A. Bramati, G. Gigli, and D. Sanvitto, arXiv:1201.4071 [cond-mat.mes-hall] (2012).

[17] P. Borri, W. Langbein, U. Woggon, J. R. Jensen, and J. M. Hvam, Phys. Rev. B **63**, 035307 (2001).

[18] J. R. Jensen, J. M. Hvam, and W. Langbein, J. Appl. Phys. **86**, 2584 (1999).

[19] J. R. Jensen, P. Borri, W. Langbein, and J. M. Hvam, Appl. Phys. Lett. **76**, 3262 (2000).

[20] J. M. Zajac, W. Langbein, M. Hugues, and M. Hopkinson, Phys. Rev. B **85**, 165309 (2012).

[21] W. Langbein, Rivista del nuovo cimento **33**, 255 (2010).

[22] W. Langbein, Journal of Physics Condensed Matter **16**, S3645 (2004).

[23] W. Langbein, P. Borri, U. Woggon, V. Stavarache, D. Reuter, and A. D. Wieck, Phys. Rev. B **70**, 033301 (2004).

[24] D. D. Solnyshkov, I. A. Shelykh, N. A. Gippius, A. V. Kavokin, and G. Malpuech, Phys. Rev. B **77**, 045314 (2008).

[25] A. Huynh, J. Tignon, O. Larsson, P. Roussignol, C. Delalande, R. André, R. Romestain, and L. S. Dang, Phys. Rev. Lett. **90**, 106401 (2003).

[26] N_{LP} was calculated using the lower polariton lifetime $\tau = \hbar/\gamma_{\mathrm{LP}}$, it is evaluated for each excitation parameters and given in the figures captions. DBR top mirror transmission for $\gamma_{\mathrm{cav}} = 300\,\mu$eV was calculated as $T = 0.3\%$

---

[*] Electronic address:joanna.m.zajac@gmail.com

[1] A. Kavokin, J. Baumberg, G. Malpuech, and F. Laussy,
Microcavities, Series on Semiconductor Science and Technology (OUP Oxford, 2007), ISBN 9780191620737.

[2] R. W. Boyd, *Nonlinear Optics* (Academic Press, 2008).

[3] P. G. Savvidis, J. J. Baumberg, R. M. Stevenson, M. S. Skolnick, D. M. Whittaker, and J. S. Roberts, Phys. Rev. Lett. **84**, 1547 (2000).

[4] P. G. Savvidis, C. Ciuti, J. J. Baumberg, D. M. Whittaker, M. S. Skolnick, and J. S. Roberts, Phys. Rev. B **64**, 075311 (2001).

[5] A. I. Tartakovskii, D. N. Krizhanovskii, D. A. Kurysh, V. D. Kulakovskii, M. S. Skolnick, and J. S. Roberts, Phys. Rev. B **65**, 081308 (2002).

[6] V. Kohnle, Y. Léger, M. Wouters, M. Richard, M. T. Portella-Oberli, and B. Deveaud-Plédran, Phys. Rev. Lett. **106**, 255302 (2011).

[7] C. Ciuti, P. Schwendimann, and A. Quattropani, Phys. Rev. B **63, 4**, 5 (2001), parametric.

[8] C. Ciuti, P. Schwendimann, and A. Quattropani, Semicond. Sci. Technol. **18**, S279 (2003).

[9] W. Langbein, Phys. Rev. B **70**, 205301 (2004).

[10] W. Langbein, Phys. Status Solidi B **242**, 2260 (2005).

[11] S. Savasta, O. D. Stefano, V. Savona, and W. Langbein, Phys. Rev. Lett. **94**, 246401 (2005).

[12] M. Abbarchi, V. Ardizzone, T. Lecomte, A. Lemaitre, I. Sagnes, P. Senellart, J. Bloch, P. Roussignol, and J. Tignon, Phys. Rev. B **83**, 201310 (2011).

[13] V. Ardizzone, M. Abbarchi, T. Lecomte, A. Lemaitre, I. Sagnes, P. Senellart, J. Bloch, P. Roussignol, and J. Tignon, Phys. Status Solidi B **249**, 896 (2012).

[14] A. Amo, J. Lefrere, S. Pigeon, C. Adrados, C. Ciuti, I. Carusotto, R. Houdré, E. Giacobino, and A. Bramati, Nature Physics **5**, 805 (2009).

[15] E. Cancellieri, F. M. Marchetti, M. H. Szymańska, D. Sanvitto, and C. Tejedor, Phys. Rev. Lett. **108**, 065301 (2012).

[16] D. Ballarini, M. D. Giorgi, E. Cancellieri, R. Houdré, E. Giacobino, R. Cingolani, A. Bramati, G. Gigli, and D. Sanvitto, arXiv:1201.4071 [cond-mat.mes-hall] (2012).

[17] P. Borri, W. Langbein, U. Woggon, J. R. Jensen, and J. M. Hvam, Phys. Rev. B **63**, 035307 (2001).

[18] J. R. Jensen, J. M. Hvam, and W. Langbein, J. Appl. Phys. **86**, 2584 (1999).

[19] J. R. Jensen, P. Borri, W. Langbein, and J. M. Hvam, Appl. Phys. Lett. **76**, 3262 (2000).

[20] J. M. Zajac, W. Langbein, M. Hugues, and M. Hopkinson, Phys. Rev. B **85**, 165309 (2012).

[21] W. Langbein, Rivista del nuovo cimento **33**, 255 (2010).

[22] W. Langbein, Journal of Physics Condensed Matter **16**, S3645 (2004).

[23] W. Langbein, P. Borri, U. Woggon, V. Stavarache, D. Reuter, and A. D. Wieck, Phys. Rev. B **70**, 033301 (2004).

[24] D. D. Solnyshkov, I. A. Shelykh, N. A. Gippius, A. V. Kavokin, and G. Malpuech, Phys. Rev. B **77**, 045314 (2008).

[25] A. Huynh, J. Tignon, O. Larsson, P. Roussignol, C. Delalande, R. André, R. Romestain, and L. S. Dang, Phys. Rev. Lett. **90**, 106401 (2003).